Supplementary Information

A Physiologically-Based Pharmacokinetic Model for Tuberculosis Drug Disposition at Extrapulmonary Sites

Aparna Ramachandran and Chetan J. Gadgil*

1. PBPK Model Equations

Venous blood:

$$V_V \frac{dC_V}{dt} = \sum_T ((Q_T - L_T) * C_{VT}) + (L_{LN} * C_{VLN}) - Q_C * C_V$$

Arterial blood:

$$V_A \frac{dC_A}{dt} = (Q_C - L_{Lu}) * C_{VLu} - \sum_T (Q_T * C_A) \; [\boldsymbol{or} \; ((Q_C - L_{Lu}) * C_A)]$$

Lungs:

$$V_{Lu} \frac{dC_{Lu}}{dt} = Q_C * C_V - (Q_C - L_{Lu}) * C_{VLu} - (L_{Lu} - Q_{Pl}) * C_{VLu} - Q_{Pl} * C_{VLu}$$

Pleura:

$$V_{Pl} \frac{dC_{Pl}}{dt} = Q_{Pl} * C_{VLu} - Q_{Pl} * C_{Pl}$$

Non-eliminating tissues/organs with afferent lymph (Brain, Heart, Adipose, Muscle, Skin, Others):

$$V_T \frac{dC_T}{dt} = Q_T * C_A - (Q_T - L_T) * C_{VT} - L_T * C_{VT}$$

Non-eliminating tissues/organs without afferent lymph (Bone, Spleen):

$$V_T \frac{dC_T}{dt} = Q_T * C_A - Q_T * C_{VT}$$

Kidney:

$$V_{Kd} \frac{dC_{Kd}}{dt} = Q_{Kd} * C_A - (Q_{Kd} - L_{Kd}) * C_{VKd} - L_{Kd} * C_{VKd} - f_R * CL * C_A$$

Gut:

$$V_{Gu} \frac{dC_{Gu}}{dt} = Q_{Gu} * C_A - (Q_{Gu} - L_{Gu}) * C_{VGu} - L_{Gu} * C_{VGu} + k_a * A_D + k_r * A_{GL}$$

Liver:

$$V_{Li} \frac{dC_{Li}}{dt} = Q_{LA} * C_A + Q_{Sp} * C_{VSp} + (Q_{Gu} - L_{Gu}) * C_{VG} - (Q_{Li} - L_{Li}) * C_{VLi} - L_{Li} * C_{VLi} - (1 - f_R) * CL * \frac{Q_{LA} * C_A + Q_{Sp} * C_{Sp} + Q_{Gu} * C_{Gu}}{Q_{Li}}$$

Gut Lumen (GL):

$$\frac{dA_{GL}}{dt} = (1 - f_R) * CL * \frac{Q_{LA} * C_A + Q_{Sp} * C_{Sp} + Q_{Gu} * C_{Gu}}{Q_{Li}} - k_r * A_{GL} - k_F * A_{GL}$$

Lymph Node:

$$V_{LN} \frac{dC_{LN}}{dt} = \sum_T (L_T * C_{VT}) - L_{LN} * C_{VLN}$$

Drug Absorption:

$$\frac{dA_D}{dt} = -k_a * A_D$$

In this system of equations, Q_T (L/hr) is the flow rate to a tissue/organ "T", L_T (L/hr) is the lymph flow rate from tissue/organ "T", C_A (µg/mL) is the drug concentration in arterial blood, Q_{Pl} is the flow rate of the pleura, *CL* (L/hr) is total systemic clearance of the drug, F_T is the fraction of total clearance apportioned to T (if any), and C_{VT} (µg/mL) is the drug concentration exiting T with $C_{VT} = C_T/P_T$, where P_T is the tissue:blood partition co-efficient for T. Summation of blood flow rates is for all tissues except lungs. Amount of drug in tissue T is $A_T = C_T * V_T$, where V_T is the volume of T. A_D is the amount of drug input to the gut. k_a is the oral absorption rate, k_r is the rifampicin gut reabsorption rate during enterohepatic circulation, and k_F is the gut lumen transit rate

2. Objective Function Used for Minimization to Estimate Parameters

Least squares method is used by the *fitnlm* function during model calibration. Hence, the sum of squares of the offsets of experimental data points from the model simulated concentration curve is minimized, where we assign weight to certain data points. The weights are used to emphasize the *Cmax* values and are listed in Table S6. This function for *n* reported data points is:

$$\sum_{i=1}^{n} w_i (y_i - f(x_i))^2$$

y_i is the measured value of the dependent variable, $f(x_i)$ is the model predicted value and w_i is the weight assigned to i^{th} observation. The values assigned for w_i are listed in Table S6.

3. Pleural Fluid Compartment

The proposed model includes a pleural space compartment represented as extension of the lung. It receives filtrate from the lungs and drains via lymphatics, as shown in the figure here:

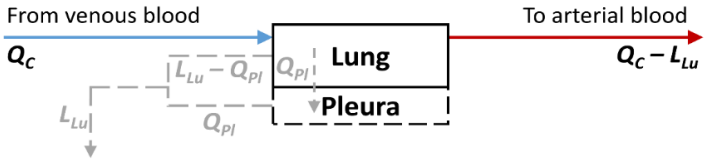

Figure: Schematic representation of entry and exit of pleural fluid. The fluid is a filtrate from the lung that enters the pleural space and is drained from here by lymphatics and leaves the lung.

We consider that the filtrate goes from the lung (flow rate Q_{Pl}) to the pleural space, and is then drained by the lymphatics (flow rate Q_{Pl}) and exits the lung with the lymph flow rate L_{Lu}. We represent this physiology using the following equation:

$$V_{Pl}\frac{dC_{Pl}}{dt} = Q_{Pl} * C_{VLu} - Q_{Pl} * C_{Pl}$$

V_{Pl} is the volume of the pleural space compartment, C_{Pl} is the drug concentration in this compartment, Q_{Pl} is flow rate of pleural fluid, and C_{VLu} is the drug concentration exiting the lung.

Our representation is based on reports that pleural fluid is a microvascular filtrate flowing in through the parietal pleural capillaries[1,2]. While disagreement exists regarding the role of visceral pleural capillaries and interstitial lymphatics in the absorption of pleural liquid, we assume that pleural liquid is removed from this space mainly through lymphatic stomata in the parietal pleura[2,3]. Rupture of a sub-pleural caseous focus in the lung into the pleural space is thought to cause pleural TB as it introduces bacteria and mycobacterial antigens into this space[4].

After simulations, when compared with literature data, values of the correlation coefficient, *r*, for rifampicin is 0.07, for ethambutol is 0.58, for isoniazid is 0.07 (fast) and 0.26 (slow) and, for pyrazinamide is 0.9.

4. Lymph Node Compartment

To our knowledge, the integration of a lymph node compartment is a novel addition to the study of tuberculosis using PBPK. Many studies have incorporated a lymph node compartment in their PBPK model to evaluate the pharmacokinetics of different substances such as peptides[5], monoclonal antibodies[6,7], nanoparticles[8,9] as well as small molecules[10]. A recent PBPK study based on non-human primates has demarcated the lymph node network into five major regions, which then drain into the thoracic duct[11].

5. Relation of Pyrazinamide Activity to Environmental pH and its Effect on Treatment

Environmental pH has been seen to play an important role in the sterilizing activity of pyrazinamide. Pyrazinamide's anti-bacterial activity has been shown to increase with decreasing pH values[12]. Pyrazinamide is thought to target non- or slowly-reproducing bacteria in acidic compartments such as the macrophage phagosome[13,14]. While immature phagosomes have a pH of 6.2, post bacilli internalization by macrophage, acidification occurs, resulting in a phagosomal pH of pH 4.5 to 5.0[15]. However, this notion is contradicted by the finding that macrophage vesicles containing *M. Tuberculosis* bacteria were not acidic[16]. It has also been suggested that the drug exhibits antimicrobial activity against extracellular slow-replicating bacteria in the epithelial lining fluid[17]. Poor treatment response to pyrazinamide in animal infection models such as mice and guinea pigs, with neutral to alkaline lesion pH, provide further evidence in favor of the enhanced activity of the drug in acidic conditions[14,15]. This observed higher pH in TB lesions in guinea pig and murine models does not appear to be an impediment to treatment with pyrazinamide in humans though, as shown in a study by Kempker et al. where a majority of the lesion samples studied by them (8 out of 10 patients) had an acidic pH (≤ 5.5)[18]. As stated by Srivastava et al., pH in human TB cavities varies around 5.5, while that in murine TB models is higher[19]. This is a probable cause for differential outcomes in the two cases.

6. Comparison of Model Predictions to Caseum MBC90 Values

We compare our model predictions in the lung tissue and at EPTB sites with the caseum bacteria MBC90 values determined in two studies[20,21]. These are illustrated in Figure S3 and Figure S4 here. The MBC90 values taken are:

- Rifampicin: 6.58 µg/mL
- Ethambutol: 104.61 µg/mL
- Isoniazid: 17.55 µg/mL
- Pyrazinamide: 63.03 µg/mL

In the lung tissues, as shown in Figure S3, in case of rifampicin, the drug crosses the MBC90 concentration albeit for a much shorter duration compared to the critical concentration. For isoniazid, both fast and slow metabolizers fail to achieve MBC90 concentrations. In case of pyrazinamide too, MBC90 concentration is not crossed.

At EPTB sites, as shown in Figure S4, simulated rifampicin concentrations in the lymph nodes, kidney and liver reach concentrations above MBC90. Simulated isoniazid (both cases) and pyrazinamide concentrations in none of the EPTB sites achieves concentrations higher than the MBC90.

7. Supplementary Tables

Table S1[†]**:** A summary of relevant whole-body PBPK models for adults incorporating first-line anti-TB drugs

	Drug	Type of TB	Features of the Model	References
1	Isoniazid	Pulmonary	• Describes NAT2-dependent pharmacokinetics of isoniazid and its metabolites • Includes acetylator status (fast,intermediate, slow)	23
2	Isoniazid	Pulmonary	• Employs two coupled PBPK models:one for a lactating mother and one for her infant to study drug exposure in the infant from drug intake by the mother • Includes acetylator status (fast and slow)	24
3	Isoniazid	Pulmonary	• Assessment of potential drug-druginteractions with CYP2C19 and CYP3A4 substrates • Includes acetylator status (fast and slow)	25
4	Ethambutol	Pulmonary	• Considers scenarios that reflect different stages of PBPK model development to evaluate drug PK	26
5	Rifampicin	Pulmonary	• Recognizes and models differences in rifampicin pharmacokinetics aftera single dose in healthy, TB and cirrhosis populations	27

[†]In these models, human physiology is described by representing organs and tissues as compartments. The number of compartments varies, depending on the modelling approach adopted. Each compartment can be homogenous and well-stirred or consist of sub-compartments. A notable model is the representation of the lung as a multi-compartment permeability-limited organ[22]. These PBPK studies simulate the time-dependent concentrations of a single drug[23–28], as well as multiple drugs[22,29–32], for first-line and many second- and third-line anti-TB drugs. The models that study first-line drugs do not include EPTB sites as their focus is pulmonary TB. To our knowledge, only one study models EPTB treatment through a PBPK model[28].

6	Rifampicin, Ethambutol	Pulmonary	• Structured model with two organisms: lactating mother and nursing infant	29
7	Rifampicin, Isoniazid, Pyrazinamide, Ethambutol	Pulmonary	• Properties predicted from mice were used to deduce parameters and predict lung:plasma ratio in humans which were compared to biopsy data from patients	30
8	Bedaquiline, Delamanid, Isoniazid, Rifapentine	Pulmonary	• Simulates the long-acting administration of select anti-TBdrugs for LTBI treatment • Includes acetylator status	31
10	Rifampicin, Ethambutol, Isoniazid, Itraconazole, Erythromycin, Clarithromycin, Pyrazinamide	Pulmonary (Lungs)	• Incorporates a multi-compartment permeability-limited lung model instead of a single homogeneous lung compartment	22
11	Bedaquiline, Clofazimine, Cycloserine, Isoniazid Ethambutol, Ethionamide, Kanamycin, Pyrazinamide, Rifampicin, Linezolid	Pulmonary (Lungs)	• Model accuracy assessed using drug plasma concentrations and lung tissue concentrations	32

Table S2: Physiological parameters for the assumed male individual

Parameter	**Value**	**References**
Body weight	70 kg	Assumption
Cardiac output (Q_C)	5200 mL/min	33
Afferent lymph flow rate	8 L/day	34
Gut lumen transit rate (k_F)	0.252 hr^{-1}	35

Table S3: Tissue-wise physiological parameter values

Organ/Tissue	**Symbol**	**Volume**[6,33,36] (as fraction of Body Weight)	**Blood Flow Rate**[33,35] (as fraction of Cardiac Output)	**Lymph Flow Rate**[37] (as fraction of Afferent Lymph Flow)
Lungs	Lu	0.0076	-	0.03
Brain	Br	0.02	0.12	0.0105
Adipose	Ad	0.2142[a]	0.05	0.128
Heart	Hr	0.0047	0.04	0.01
Muscle	Mu	0.4	0.17	0.16
Bone	Bo	0.1429[a]	0.05	0
Skin	Sk	0.0371	0.05	0.0703
Kidney	Kd	0.0044	0.19	0.085
Spleen	Sp	0.0026	77/5200[e]	0
Gut	Gu	0.0171	1100/5200[e]	0.12
Liver	Li	0.0257	$Q_{LA} + Q_{Gu} + Q_{Sp}$	0.33
Hepatic Artery	LA	-	0.06	-
Lymph Node	LN	0.274/70[b]	-	-
Arterial Blood	A	1.8/70[c]	-	-
Venous Blood	V	3.6/70[c]	-	-
Others	Oth	0.04264[d]	0.04365[f]	0.0562[g]
Pleura	Pl	0.3 mL $kg^{-1,3}$*	0.15 mL kg^{-1} $h^{-1,3}$*	-

a: Density = Mass/Volume. We assume that Density ≈ 1 g/cm^3 and so Mass ≈ Volume, except foradipose where density = 0.916 g/cm^3 and for bone where density = 1.92 g/cm^3

b: Taken from Shah & Betts, 2012 (Combined volume of LNs = 274 mL)

c: Taken from Igari et al. (Volume of arterial blood = 1.8 L, venous blood = 3.6 L)

d: Others = 1 – (Sum of other compartments) = 1 – 0.9576 = 0.0424

e: Taken from Davies & Morris, 1993

f: Others = 1 – (Sum of other compartments) = 1 – 0.95635 = 0.04365 (Pleura fraction is considered negligible)

g: Others = 1 – (Sum of other compartments) = 1 – 0.9438 = 0.0562

*: Not a fraction

Table S4: Chemical and biological properties of the 4 first-line anti-TB drugs

	Rifampicin	**Ethambutol**	**Isoniazid**	**Pyrazinamide**[a]
Compound type	Zwitterion[38] (group 1)	Diprotic base[22]	Monoprotic base[22]	Neutral[22]
Acid dissociation constant (pKa)	pKa1 = 1.7, pKa2 = 7.9[38]	pKa1 = 6.5, pKa2 = 9.55[22]	1.82[22]	0.5[39]
logPo:w	2.7[38]	-0.3[40]	-0.7[41]	-0.6[39]
logPvo:w	1.7	-1.7	-2.1	-2
BP	0.9[42]	0.99[#]	1*	1*
Kpu_{BC}	5.2	1.30[43]	1.1	1.1
Ka_{BC}	7	1.31	–	–
fu	0.15[44]	0.75[22]	0.95[22]	0.9[22]
fR	0.07[45]	0.79[45]	Fast: 0.07[46]	0.09[45]
			Slow: 0.29[46]	

a: Pyrazinamide is hydrophilic nature[47]. Lipoproteins usually binds with hydrophobic drugs[48]. Hence, it is assumed that pyrazinamide interacts majorly with albumin instead of lipoproteins.

logPo:w – n-octanol:water logP

logPvo:w – vegetable oil:water logP is required to estimate adipose tissue Kp and is calculated using the linear regression relationship proposed by Leo et al.[49] between logPo:w and logPvo:w as experimental values were not found. The equation used here is an adaptation of this relationship, by Poulin and Theil[50], *logPvo:w = 1.1115 * logPo:w − 1.35*

BP – Blood:plasma ratio of the drug

Kpu_{BC} – Blood cell:plasma water unbound drug concentration ratio. Is calculated[51] as *(H – 1 + BP)/(fu*H)* where haematocrit H is taken to be 0.45[51], except for ethambutol for which experimental value is available

Ka_{BC} – Ka is the association constant of basic/zwitterionic drugs with acidic phospholipids of a tissue. Ka_{BC} corresponds to Ka for blood cells and is calculated using Kpu_{BC}[52]. Ka values for drugs are not available readily and hence are approximated as KaBC.

fu – fraction of drug unbound in the plasma

fR – fractional renal clearance

*: BP value for isoniazid and pyrazinamide were assumed to be 1. In P_T calculation, the B:P (blood/plasma partition coefficient) for isoniazid and pyrazinamide have been set to 1 as this experimental data is unavailable in literature. This is based on the reported assumption that for drugs that are distributed homogenously into tissues, B:P can be taken to be 1[50].

#: BP value was calculated from Kpu_{BC}

Table S5: Tissue-wise calculated partition coefficient values

Organ/Tissue	Rifampicin	Ethambutol	Isoniazid	Pyrazinamide
Lungs	1.7115	4.3966	0.7662	0.7381
Brain	0.2285	1.8054	0.7537	0.7184
Adipose	0.1885	0.4625	0.1543	0.1503
Heart	1.0158	3.0623	0.7551	0.7243
Muscle	0.6949	2.7093	0.7208	0.6868
Bone	0.3157	1.3765	0.4330	0.4163
Skin	0.6265	1.9938	0.6675	0.6496
Kidney	2.1725	5.3375	0.7441	0.7127
Spleen	1.3950	4.0004	0.7605	0.7260
Gut	1.0781	3.2051	0.7429	0.7140
Liver	1.9646	5.0703	0.7212	0.6887
Lymph Node	1.2081	3.6743	0.7556	0.7210
Others[a]	1.00470	3.1337	0.7435	0.7133

a: Median of all other values

Table S6: Weights assigned to different experimental data points during model calibration

Rifampicin												
Fig. 2	Acocella, 1978											
	1	2	3	4	5	6	7	8				
	0.0238	0.0238	0.2281	0.0238	0.0238	0.0238	0.0238	0.0238				
	Furesz, 1970											
	1	2	3	4	5	6						
	0.4363	0.0238	0.0238	0.0238	0.0238	0.0738						
Ethambutol												
Fig. 2	Strauch et al., 2011 (Etb-91-400B)											
	1	2	3	4	5	6	7	8	9	10	11	
	0.0208	0.0208	0.0208	0.0208	0.3128	0.0208	0.0208	0.0208	0.0208	0.2083	0.0208	
	Strauch et al., 2011 (Etb-ref-400)											
	1	2	3	4	5	6	7	8	9	10		
	0.0208	0.0208	0.0208	0.0208	0.0208	0.1045	0.0208	0.0208	0.0208	0.0208		
Isoniazid (FA)												
Fig. 2	Gallicano et al., 1994											
	1	2	3	4	5	6	7	8	9	10	11	12
	0.0400	0.3500	0.0400	0.0400	0.0400	0.0400	0.0400	0.0400	0.0400	0.0400	0.0400	0.2500
Isoniazid (SA)												
Fig. 2	Gallicano et al., 1994											
	1	2	3	4	5	6	7	8	9	10	11	12	13	14
	0.0357	0.5359	0.0357	0.0357	0.0357	0.0357	0.0357	0.0357	0.0357	0.0357	0.0357	0.0357	0.0357	0.0357

Table S7: Predicted PK parameters for each drug

Drug		Absorption rate, k_a (h^{-1})	Systemic Clearance, CL ($L\ h^{-1}$)
Rifampicin		1.07	7.79
Ethambutol		0.22	49.99
Isoniazid	Fast	2.86	24.56
	Slow	4.11	9.16
Pyrazinamide		1.36	4.10

8. Supplementary Figures

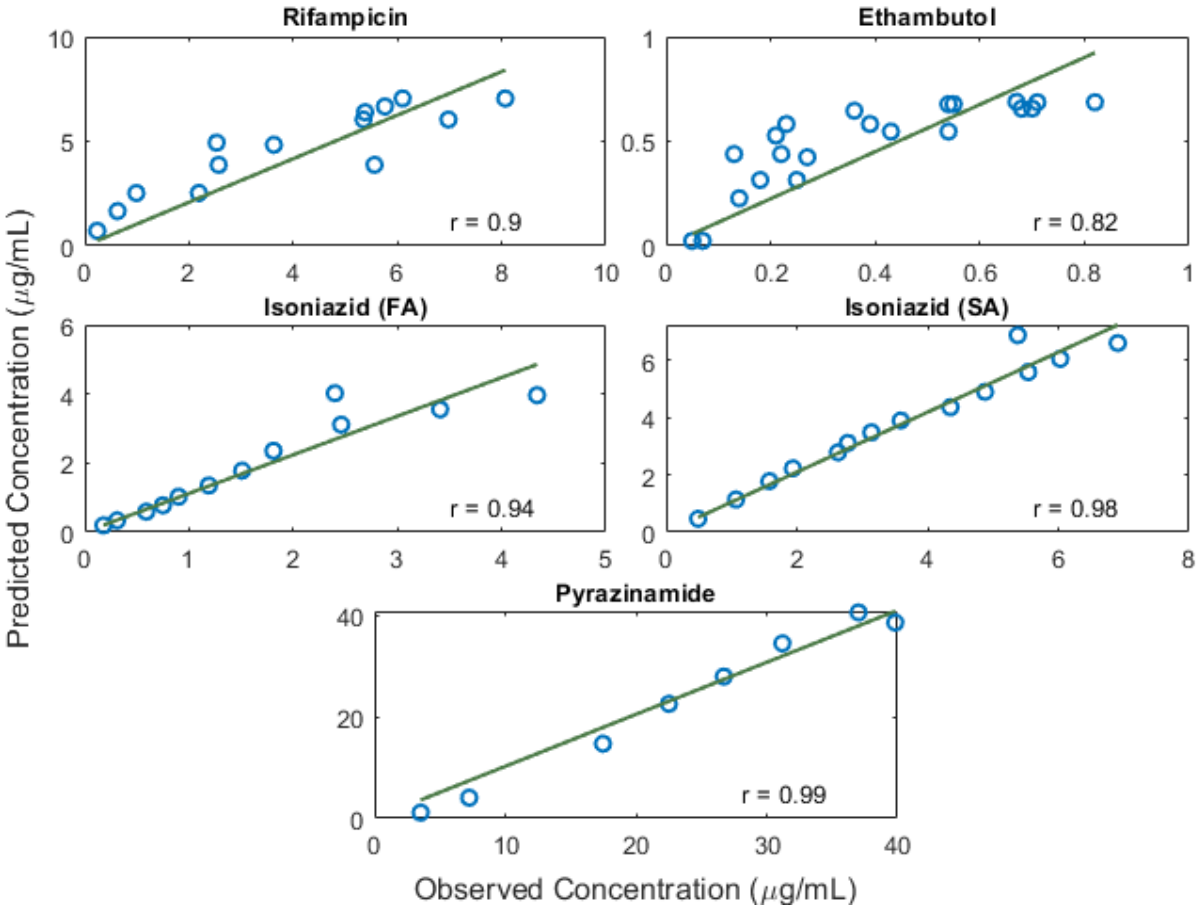

Figure S1: Model Calibration – Goodness-of-fit plots for predicted and reported plasma concentrations for oral doses of rifampicin (450 mg), ethambutol (400 mg), isoniazid (300 mg)and pyrazinamide (2000 mg). Concentration vs time predictions are shown in Figure 2. 'r' is the correlation coefficient.

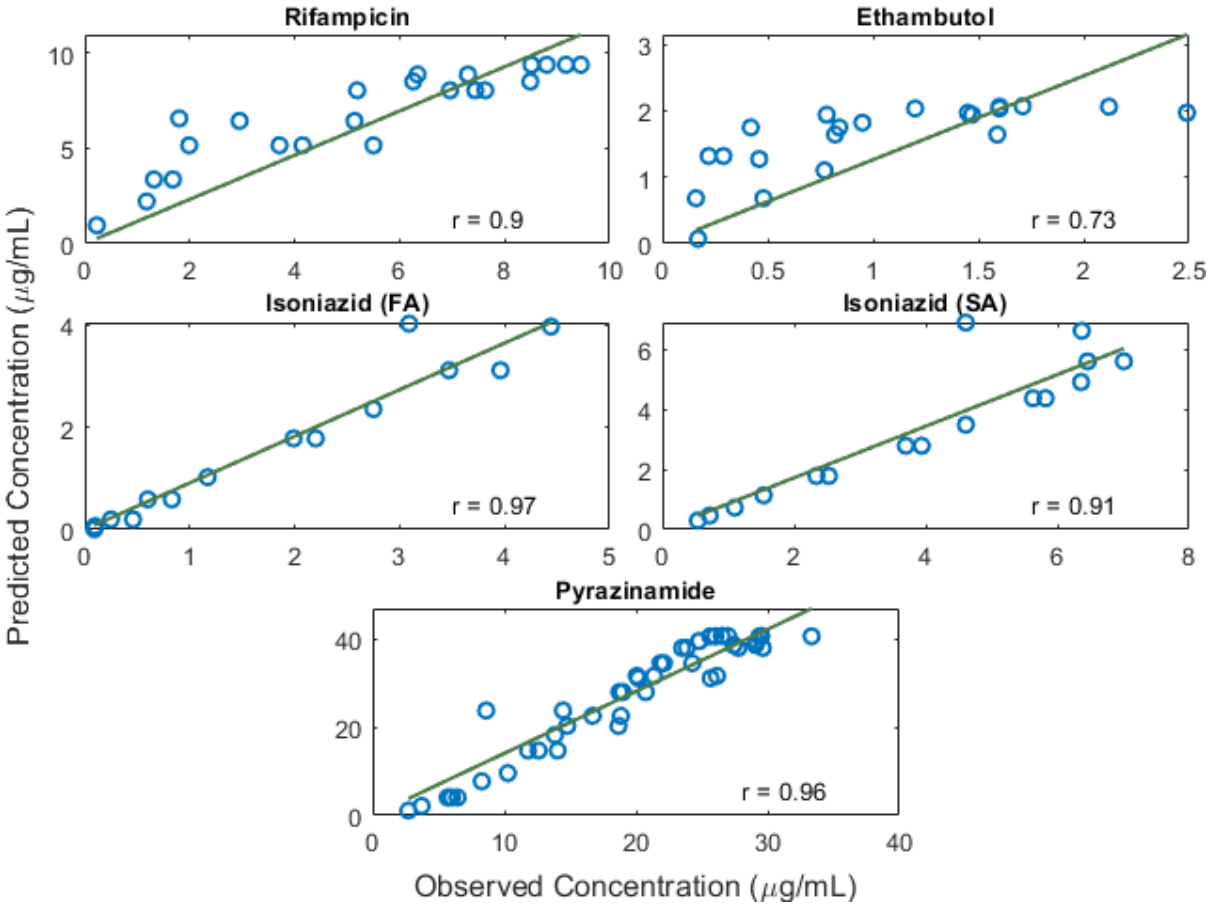

Figure S2: Model Validation – Goodness-of-fit plots for predicted and observed drug plasma concentrations in simulations. Oral doses of rifampicin (600 mg), ethambutol (1200 mg), isoniazid (300 mg) and pyrazinamide (1500 mg) were simulated. Concentration vs time predictions are shown in Figure 3. 'r' is the correlation coefficient.

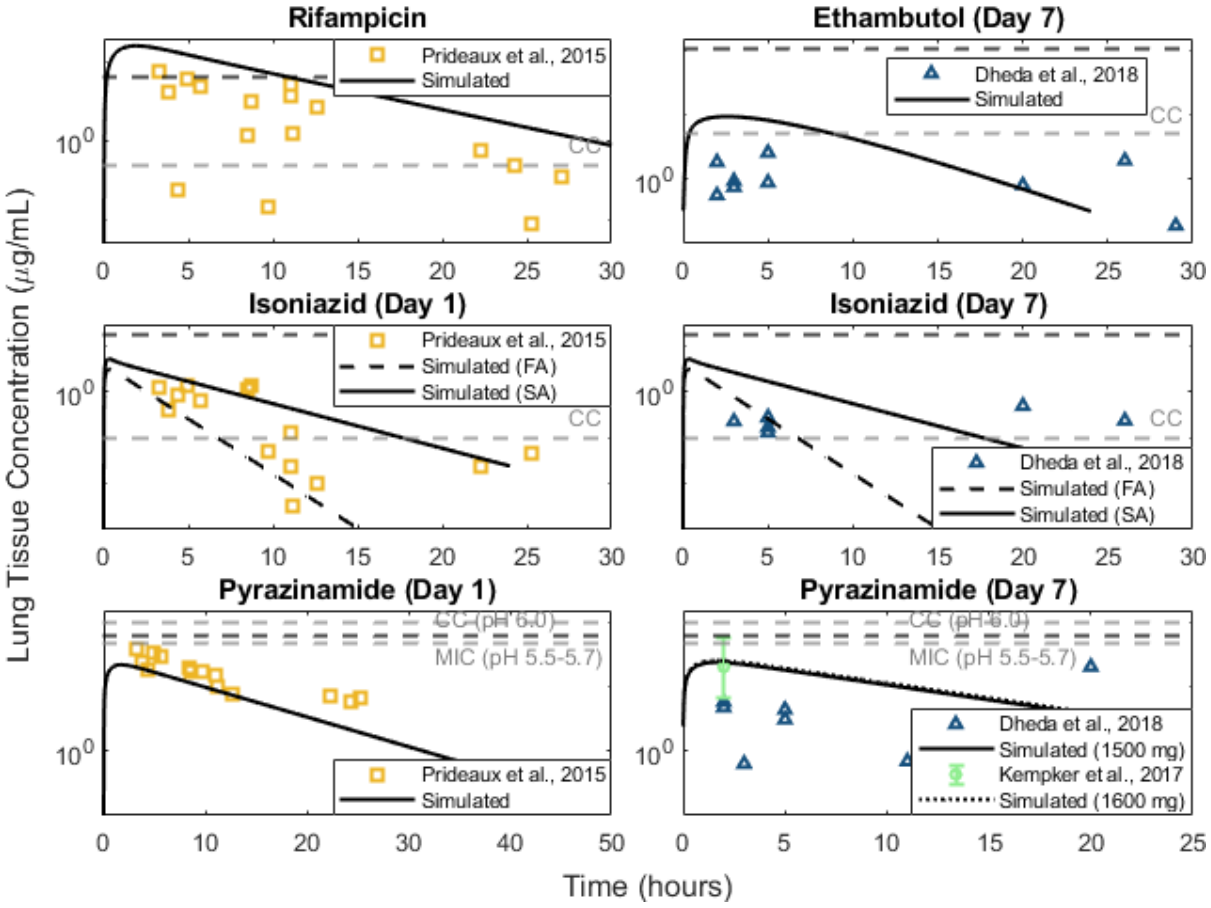

Figure S3: Simulated lung tissue drug concentrations for oral doses of rifampicin (600 mg), ethambutol (1200 mg), isoniazid (300 mg) and pyrazinamide (1500 mg and 1600 mg) plotted along with reported concentration data for each drug dose are plotted in comparison to the drug's critical concentration and caseum MBC90 values. Day 1 concentrations are simulated for rifampicin, isoniazid and pyrazinamide while day 7 concentrations for ethambutol, isoniazid and pyrazinamide are simulated as the reported data they are compared to in the right panel are derived from studies that measure drug concentrations in the tissue after daily administration. We assume that *Cmax* reaches a steady state value by then and use day 7 to represent the long-term daily profile of drug concentration. Values of the correlation coefficient, *r*, for rifampicin is 0.65, for ethambutol is 0.05, for isoniazid after single dose administration is 0.50 (fast) and 0.62 (slow) and after continuous administration is -0.39 (fast) and -0.58 (slow) and, for pyrazinamide after single dose administration is 0.88 and after continuous administration is -0.45. Kempker et al. report a median tissue concentration and this data is compared to simulations after a 1600 mg dose (dashed line). The grey dashed line represents the critical concentration of each drug (also MIC at pH 5.5-5.7 for PYZ) and the black dashed line represents the caseum MBC90 values.

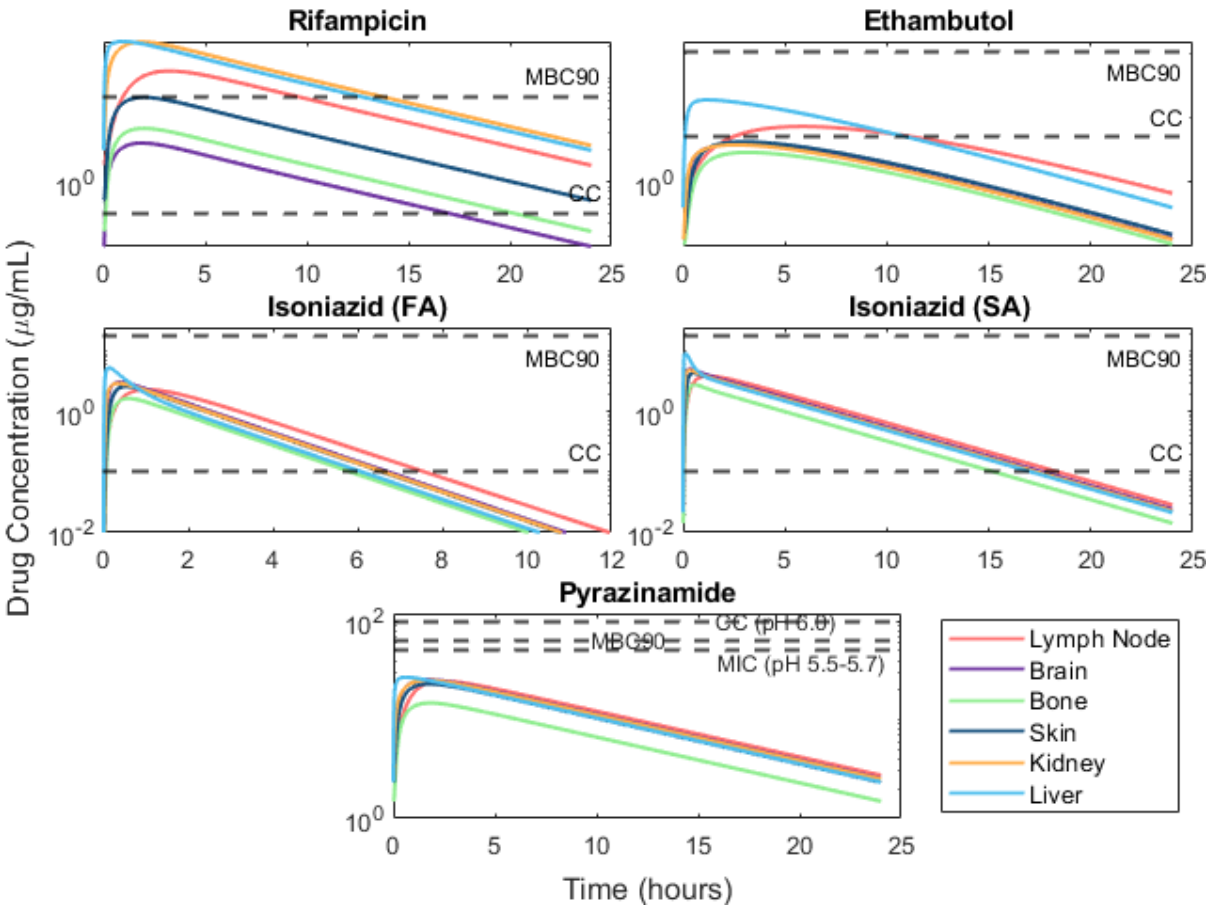

Figure S4: Simulated day 7 drug concentrations at various sites of EPTB for recommended oral doses of rifampicin (600 mg), ethambutol (1200 mg), isoniazid (300 mg) and pyrazinamide (1600 mg) compared to the critical concentration (and MIC at pH 5.5-5.7 for PYZ) and caseum MBC90 values of each drug. We assume that *Cmax* reaches a steady state value by then and use day 7 to represent the long-term daily profile of drug concentration.

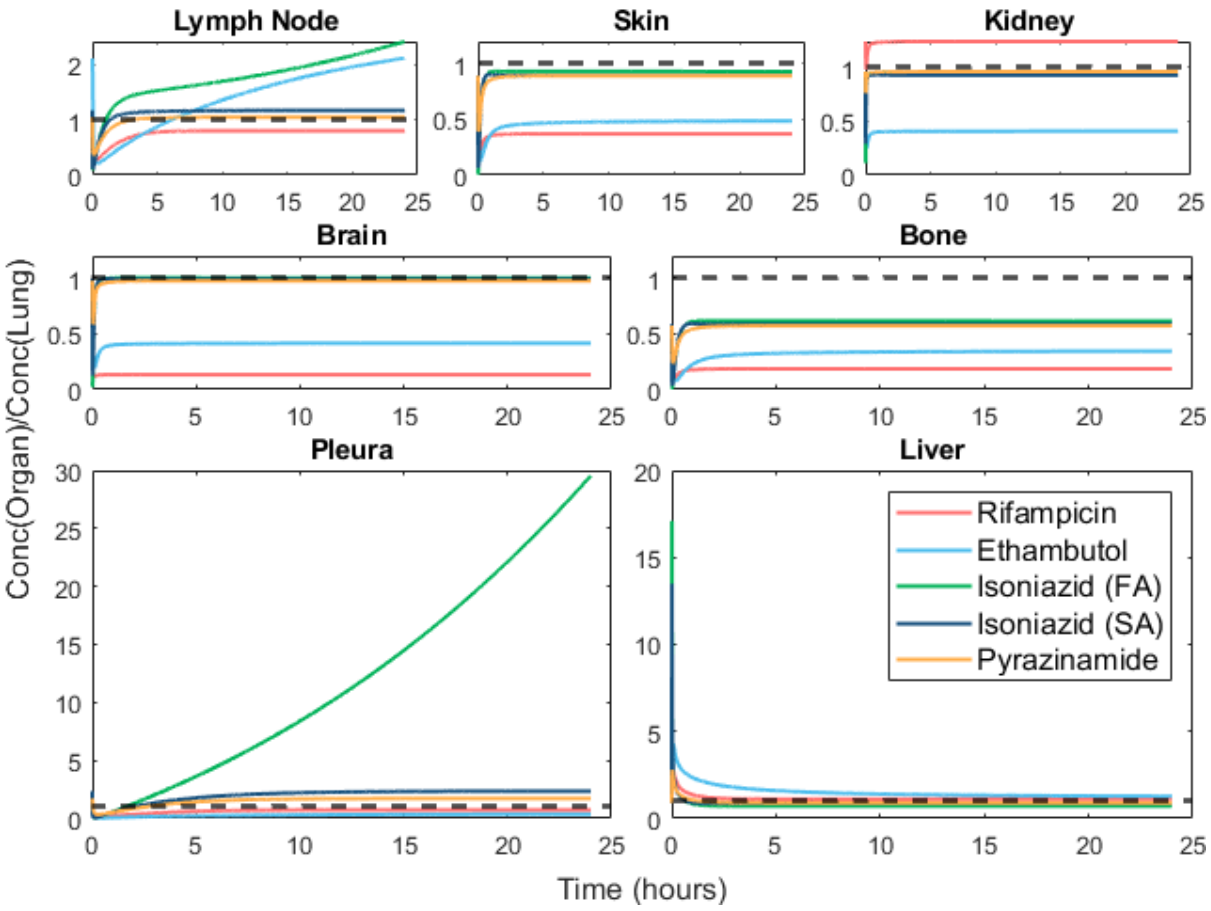

Figure S5: Ratio of time-dependent drug concentrations at different EPTB sites to that in the lung compartment after recommended oral doses of rifampicin (600 mg), ethambutol (1200 mg), isoniazid (300 mg) and pyrazinamide (1600 mg) . The dashed line indicates a ratio of 1.

References

1. Zocchi L. Physiology and pathophysiology of pleural fluid turnover. *Eur Respir J*. 2002;20(6):1545-1558. doi:10.1183/09031936.02.00062102

2. Lai-Fook SJ. Pleural mechanics and fluid exchange. *Physiol Rev*. 2004;84(2):385-410. doi:10.1152/physrev.00026.2003

3. Miserocchi G. Physiology and pathophysiology of pleural fluid turnover. *Eur Respir J*. 1997;10(1):219-225.

4. Cohen LA, Light RW. Tuberculous Pleural Effusion. *Turk Thorac J*. 2015;16(1):1-9. doi:10.5152/ttd.2014.001

5. Offman E, Phipps C, Edginton AN. Population physiologically-based pharmacokinetic model incorporating lymphatic uptake for a subcutaneously administered pegylated peptide. *Silico Pharmacol*. 2016;4:3. doi:10.1186/s40203-016-0018-5

6. Shah DK, Betts AM. Towards a platform PBPK model to characterize the plasma and tissue disposition of monoclonal antibodies in preclinical species and human. *J Pharmacokinet Pharmacodyn*. 2012;39(1):67-86. doi:10.1007/s10928-011-9232-2

7. Urva SR, Yang VC, Balthasar JP. Physiologically based pharmacokinetic model for T84.66: a monoclonal anti-CEA antibody. *J Pharm Sci*. 2010;99(3):1582-1600. doi:10.1002/jps.21918

8. Aborig M, Malik PRV, Nambiar S, et al. Biodistribution and Physiologically-Based Pharmacokinetic Modeling of Gold Nanoparticles in Mice with Interspecies Extrapolation. *Pharmaceutics*. 2019;11(4):179. doi:10.3390/pharmaceutics11040179

9. Dogra P, Butner JD, Ruiz Ramírez J, et al. A mathematical model to predict nanomedicine pharmacokinetics and tumor delivery. *Comput Struct Biotechnol J*. 2020;18:518-531. doi:10.1016/j.csbj.2020.02.014

10. Scholz EMB, Cao Y, Kashuba ADM. A cross-species comparison of antiretroviral penetration into lymph nodes using novel physiologically based pharmacokinetic models. *J Antimicrob Chemother*. 2021;76(11):2890-2893. doi:10.1093/jac/dkab298

11. Perazzolo S, Shireman LM, Shen DD, Ho RJY. Physiologically Based Pharmacokinetic Modeling of 3 HIV Drugs in Combination and the Role of Lymphatic System after Subcutaneous Dosing. Part 1: Model for the Free-Drug Mixture. *J Pharm Sci*. 2022;111(2):529-541. doi:10.1016/j.xphs.2021.10.007

12. Salfinger M, Heifets LB. Determination of pyrazinamide MICs for Mycobacterium tuberculosis at different pHs by the radiometric method. *Antimicrob Agents Chemother*. 1988;32(7):1002-1004. doi:10.1128/AAC.32.7.1002

13. Rohde K, Yates RM, Purdy GE, Russell DG. Mycobacterium tuberculosis and the environment within the phagosome. *Immunol Rev*. 2007;219(1):37-54. doi:10.1111/j.1600-065X.2007.00547.x

14. Lamont EA, Baughn AD. Impact of the host environment on the antitubercular action of pyrazinamide. *EBioMedicine*. 2019;49:374-380. doi:10.1016/j.ebiom.2019.10.014

15. Lamont EA, Dillon NA, Baughn AD. The Bewildering Antitubercular Action of Pyrazinamide. *Microbiol Mol Biol Rev*. 2020;84(2):e00070-19. doi:10.1128/MMBR.00070-19

16. Crowle AJ, Dahl R, Ross E, May MH. Evidence that vesicles containing living, virulent Mycobacterium tuberculosis or Mycobacterium avium in cultured human macrophages are not acidic. *Infect Immun*. 1991;59(5):1823-1831. doi:10.1128/iai.59.5.1823-1831.1991

17. Gumbo T, Dona CSWS, Meek C, Leff R. Pharmacokinetics-Pharmacodynamics of Pyrazinamide in a Novel In Vitro Model of Tuberculosis for Sterilizing Effect: a Paradigm for Faster Assessment of New Antituberculosis Drugs. *Antimicrob Agents Chemother*. 2009;53(8):3197-3204. doi:10.1128/AAC.01681-08

18. Kempker RR, Heinrichs MT, Nikolaishvili K, et al. Lung Tissue Concentrations of Pyrazinamide among Patients with Drug-Resistant Pulmonary Tuberculosis. *Antimicrob Agents Chemother*. 61(6):e00226-17. doi:10.1128/AAC.00226-17

19. Srivastava S, Pasipanodya JG, Gumbo T. pH Conditions under Which Pyrazinamide Works in Humans. *Antimicrob Agents Chemother*. 61(9):e00854-17. doi:10.1128/AAC.00854-17

20. Sarathy JP, Via LE, Weiner D, et al. Extreme Drug Tolerance of Mycobacterium tuberculosis in Caseum. *Antimicrob Agents Chemother*. 2018;62(2):e02266-17. doi:10.1128/AAC.02266-17

21. Sarathy JP, Xie M, Jones RM, et al. A Novel Tool to Identify Bactericidal Compounds against Vulnerable Targets in Drug-Tolerant M. tuberculosis found in Caseum. Projan SJ, ed. *mBio*. 2023;14(2):e00598-23. doi:10.1128/mbio.00598-23

22. Gaohua L, Wedagedera J, Small BG, et al. Development of a Multicompartment Permeability-Limited Lung PBPK Model and Its Application in Predicting Pulmonary Pharmacokinetics of Antituberculosis Drugs. *CPT Pharmacomet Syst Pharmacol*. 2015;4(10):605-613. doi:https://doi.org/10.1002/psp4.12034

23. Cordes H, Thiel C, Aschmann HE, Baier V, Blank LM, Kuepfer L. A Physiologically Based Pharmacokinetic Model of Isoniazid and Its Application in Individualizing Tuberculosis Chemotherapy. *Antimicrob Agents Chemother*. 2016;60(10):6134-6145. doi:10.1128/AAC.00508-16

24. Garessus EDG, Mielke H, Gundert-Remy U. Exposure of Infants to Isoniazid via Breast Milk After Maternal Drug Intake of Recommended Doses Is Clinically Insignificant Irrespective of Metaboliser Status. A Physiologically-Based Pharmacokinetic (PBPK) Modelling Approach to Estimate Drug Exposure of Infants via Breast-Feeding. *Front Pharmacol*. 2019;10:5. doi:10.3389/fphar.2019.00005

25. Balhara A, Singh S. PBPK Analysis to Study the Impact of Genetic Polymorphism of NAT2 on Drug-Drug Interaction Potential of Isoniazid. *Pharm Res*. 2021;38(9):1485-1496. doi:10.1007/s11095-021-03095-9

26. Carrara L, Magni P, Teutonico D, Pasotti L, Della Pasqua O, Kloprogge F. Ethambutol disposition in humans: Challenges and limitations of whole-body physiologically-based pharmacokinetic modelling in early drug development. *Eur J Pharm Sci*. 2020;150:105359. doi:10.1016/j.ejps.2020.105359

27. Rasool MF, Khalid S, Majeed A, et al. Development and Evaluation of Physiologically Based Pharmacokinetic Drug–Disease Models for Predicting Rifampicin Exposure in Tuberculosis and Cirrhosis Populations. *Pharmaceutics*. 2019;11(11):578. doi:10.3390/pharmaceutics11110578

28. Shibata M, Masuda M, Sasahara K, et al. Prediction of Human Pharmacokinetic Profiles of the Antituberculosis Drug Delamanid from Nonclinical Data: Potential Therapeutic Value against Extrapulmonary Tuberculosis. *Antimicrob Agents Chemother*. 65(8):e02571-20. doi:10.1128/AAC.02571-20

29. Partosch F, Mielke H, Stahlmann R, Gundert-Remy U. Exposure of Nursed Infants to Maternal Treatment with Ethambutol and Rifampicin. *Basic Clin Pharmacol Toxicol*. 2018;123(2):213-220. doi:10.1111/bcpt.12995

30. Muliaditan M, Teutonico D, Ortega-Muro F, Ferrer S, Pasqua OD. Prediction of lung exposure to anti-tubercular drugs using plasma pharmacokinetic data: implications for dose selection. *Eur J Pharm Sci*. Published online March 4, 2022:106163. doi:10.1016/j.ejps.2022.106163

31. Rajoli RK, Podany AT, Moss DM, et al. Modeling the long-acting administration of anti-tuberculosis agents using PBPK – a proof of concept study. *Int J Tuberc Lung Dis Off J Int Union Tuberc Lung Dis*. 2018;22(8):937-944. doi:10.5588/ijtld.17.0515

32. Humphries H, Almond L, Berg A, et al. Development of physiologically-based pharmacokinetic models for standard of care and newer tuberculosis drugs. *CPT Pharmacomet Syst Pharmacol*. 2021;10(11):1382-1395. doi:10.1002/psp4.12707

33. Brown RP, Delp MD, Lindstedt SL, Rhomberg LR, Beliles RP. Physiological parameter values for physiologically based pharmacokinetic models. *Toxicol Ind Health*. 1997;13(4):407-484. doi:10.1177/074823379701300401

34. Renkin EM. Some consequences of capillary permeability to macromolecules: Starling's hypothesis reconsidered. *Am J Physiol-Heart Circ Physiol*. 1986;250(5):H706-H710. doi:10.1152/ajpheart.1986.250.5.H706

35. Davies B, Morris T. Physiological parameters in laboratory animals and humans. *Pharm Res*. 1993;10(7):1093-1095. doi:10.1023/a:1018943613122

36. Igari Y, Sugiyama Y, Sawada Y, Iga T, Hanano M. Prediction of diazepam disposition in the rat and man by a physiologically based pharmacokinetic model. *J Pharmacokinet Biopharm*. 1983;11(6):577-593. doi:10.1007/BF01059058

37. Gill KL, Gardner I, Li L, Jamei M. A Bottom-Up Whole-Body Physiologically Based Pharmacokinetic Model to Mechanistically Predict Tissue Distribution and the Rate of Subcutaneous Absorption of Therapeutic Proteins. *AAPS J*. 2016;18(1):156-170. doi:10.1208/s12248-015-9819-4

38. PubChem. Rifampicin. Accessed August 18, 2021. https://pubchem.ncbi.nlm.nih.gov/compound/135398735

39. PubChem. Pyrazinamide. Accessed August 18, 2021. https://pubchem.ncbi.nlm.nih.gov/compound/1046

40. PubChem. Ethambutol. Accessed August 23, 2021. https://pubchem.ncbi.nlm.nih.gov/compound/14052

41. PubChem. Isoniazid. Accessed August 23, 2021. https://pubchem.ncbi.nlm.nih.gov/compound/3767

42. Loos U, Musch E, Jensen JC, Mikus G, Schwabe HK, Eichelbaum M. Pharmacokinetics of oral and intravenous rifampicin during chronic administration. *Klin Wochenschr*. 1985;63(23):1205-1211. doi:10.1007/BF01733779

43. Lee CS, Gambertoglio JG, Brater DC, Benet LZ. Kinetics of oral ethambutol in the normal subject. *Clin Pharmacol Ther*. 1977;22(5 Pt 1):615-621. doi:10.1002/cpt1977225part1615

44. Burman WJ, Gallicano K, Peloquin C. Comparative pharmacokinetics and pharmacodynamics of the rifamycin antibacterials. *Clin Pharmacokinet*. 2001;40(5):327-341. doi:10.2165/00003088-200140050-00002

45. Brunton L, Knollman B, Hilal-Dandan R. *Goodman and Gilman's The Pharmacological Basis of Therapeutics, 13th Edition*. McGraw Hill Professional; 2017.

46. Wilkins JJ, Langdon G, McIlleron H, Pillai G, Smith PJ, Simonsson USH. Variability in the population pharmacokinetics of isoniazid in South African tuberculosis patients. *Br J Clin Pharmacol*. 2011;72(1):51-62. doi:10.1111/j.1365-2125.2011.03940.x

47. Piccaro G, Poce G, Biava M, Giannoni F, Fattorini L. Activity of lipophilic and hydrophilic drugs against dormant and replicating Mycobacterium tuberculosis. *J Antibiot (Tokyo)*. 2015;68(11):711-714. doi:10.1038/ja.2015.52

48. Sobansky MR, Hage DS. Analysis of Drug Interactions with Lipoproteins by High-Performance Affinity Chromatography. *Adv Med Biol*. 2012;53:199-216.

49. Leo A, Hansch C, Elkins D. Partition coefficients and their uses. *Chem Rev*. 1971;71(6):525-616. doi:10.1021/cr60274a001

50. Poulin P, Theil F. Prediction of Pharmacokinetics Prior to In Vivo Studies. 1. Mechanism-Based Prediction of Volume of Distribution. *J Pharm Sci*. 2002;91(1):129-156. doi:10.1002/jps.10005

51. Rowland M, Tozer TN. *Clinical Pharmacokinetics: Concepts and Applications*. Williams & Wilkins; 1995.

52. Rodgers T, Leahy D, Rowland M. Physiologically based pharmacokinetic modeling 1: predicting the tissue distribution of moderate-to-strong bases. *J Pharm Sci*. 2005;94(6):1259-1276. doi:10.1002/jps.20322